Hindawi Publishing Corporation
Journal of Thermodynamics
Volume 2010, Article ID 130692, 9 pages
doi:10.1155/2010/130692

Research Article

Ideal Thermodynamic Cycle Analysis for the Meletis-Georgiou Vane Rotary Engine Concept

Demos P. Georgiou, Nikolaos G. Theodoropoulos, and Kypros F. Milidonis

Thermal Engines Laboratory, Department of Mechanical Engineering and Aeronautics, University of Patras, 26500 Rion-Patras, Greece

Correspondence should be addressed to Demos P. Georgiou, dpgeorg@mech.upatras.gr

Received 1 December 2009; Accepted 5 May 2010

Academic Editor: Pedro Jorge Martins Coelho

The Meletis-Georgiou is a patented Vane Rotary Engine concept that incorporates separate compression-expansion chambers and a modified Otto (or Miller) cycle, characterized by (Exhaust) Gas Recirculation at elevated pressures. This is implemented by transferring part of the expansion chamber volume into the compression one through the coordinated action of two vane diaphragms. This results into a very high gas temperature at the end of the compression, something that permits autoignition under all conditions for a Homogeneous Compression Ignition (HCCI) version of the engine. The relevant parametric analysis of the ideal cycle shows that the new cycle gives ideal thermal efficiencies of the order of 60% to 70% under conditions corresponding to homogeneous compression engines but at reduced pressures when compared against the corresponding Miller cycle.

1. Introduction

Vane Rotary (VR) engine concepts are nearly as old as the reciprocating mechanism. Although no patent has evolved into a widespread commercial application, new concepts are patented regularly (e.g., [1–4]). The VR concept exhibits two advantages against the conventional two or four stroke reciprocating engines.

(i) A larger number of thermodynamic cycles implemented per shaft rotation (i.e., smaller and lighter engines).

(ii) Nearly perfect radial force balance (i.e., a much smother running).

The main disadvantages involve:

(i) The "gear"-like contact between the diaphragms and the engine rotor.

(ii) The very fast implementation of the cycles.

The first leads to increased diaphragm wear rates and gas leakage. The second requires a multibarrel drum of rotating combustion chambers in order to decouple the completion of the process from the need to expand flue gases. So far, only conventional thermodynamic cycles (Otto, Diesel, Brayton, and Miler) have been proposed for VR engine geometries patented. As a result, these concepts had to employ rather complex flow channels, if the processes were to be implemented as specified by the cycles. Meletis and Georgiou were awarded a patent [1] for a new VR engine concept characterized by a fully balanced, symmetric rotor mechanism and a new thermodynamic cycle, which incorporates (Exhaust) Gas Recirculation (EGR) process at elevated pressures. The cycle attempts to address concurrently two problems: (i) the need for a high temperature at the end of the compression, in order to guarantee ignition at low equivalence mixture ratios (i.e., in strongly diluted air), and (ii) a rather small temperature at the completion of the isochoric combustion process. Both of them are well known requirements for a low NOx exhaust. The present study investigates parametrically the merits of this new cycle, concentrating on the ideal limit of the processes and the maximum to minimum temperature ratios associated with HCCI concepts. This level of cycle analysis does not provide accurate parameter values but it does give reasonable tendency estimates, something that is needed for the early design stages. Such an engine is undergoing leakage and mechanism friction testing in our Laboratory. The following

analysis was employed as the first step for the design of the detailed engine cycle.

2. The Meletis-Georgiou Concept

The Meletis-Georgiou (MG) Vane Rotary concept is illustrated in Figure 1. It consists of a circular stator inside which rotates a fully balanced Rotor. The engine design is characterized by the number of lobes it employs to create the various chambers. Figures 1(a)–1(c) illustrates a two-lobe rotor, that is, the minimum configuration that ensures a centrifugal force balance. In actual practice, however, a four-lobe rotor configuration (see Figure 1(d)) will be preferred, since this is the minimum configuration providing full dynamic balance of all radial forces (both centrifugal and gaseous). The four lobe concept will implement four thermodynamic cycles per shaft revolution, that is, eight times faster than the corresponding four stroke reciprocating engine. The engine undergoing testing in our Laboratory employs a four lobe rotor, but for reasons of simplicity the engine operation will be analyzed on the basis of a two-lobe rotor.

Most of the gas chambers implementing the thermodynamic processes in such an engine are formed by the cavities defined by the rotor outer surface, the stator inner surface, the radially moving diaphragms and the two end plates. The MG concept requires three diaphragms per two lobes. At any rotor angular position, these cavities and the corresponding diaphragms create four engine chambers. They are

(i) (V_{IN}) (the inlet volume),

(ii) (V_C) (the compression one),

(iii) (V_E) (the expansion one),

(iv) (V_{EX}) (the exhaust one).

Figure 1(a) illustrates only two chambers, called (V_T). They chambers correspond to the maximum volume created by the inner stator surface and the outer rotor one. As the shaft rotates, the diaphragms plunge inside, so that their tips are always in contact with the rotor surface. The introduction of the diaphragms splits each of the above chambers in two new cavities, so it leads to the earlier four as illustrated in Figure 1(b). An additional cavity is embedded inside the stator structure, the combustion volume, (V_{CC}). On the two sides of the combustion chamber are positioned two (of the three) diaphragms. At any moment only one of them is lowered and maintains contact with the rotor surface. The other remains embedded inside the stator, waiting for its turn. Their relative motion will be described later on. These diaphragms divide the left chamber (volume V_T) into the compression (V_C) and expansion (V_E) cavities. The third diaphragm separates the chamber on the right side into the charging (inlet) (V_{IN}) and discharging (exhaust) (V_{Ex}) cavities. Each of these cavities communicates with the atmosphere through a port. As the engine shaft turns and the diaphragms maintain contact with the rotor outer surface, the four chamber volumes vary in magnitude. Initially the combustion chamber is connected to the expansion chamber, supplying it with high-pressure flue gasses. At this stage diaphragm 1 is lowered inside, while diaphragm 2 remains inside the stator. On the left of diaphragm 1 lies the compression volume (V_C), but this is labeled as such only after the following lobe shuts the inlet port, so that the trapped air may be compressed as the rotor turns. At a certain angular position (to be defined by the cycle optimization processes) diaphragm 1 is lifted, while diaphragm 2 is lowered inside and contacts the rotor surface. This changeover means that now the hot flue gasses within (V_{CC}) and the section of the expansion volume between diaphragms 1 and 2 become part of the compression volume. The rest of the expansion cavity gasses continue to expand until the rotor tip uncovers the exhaust port. At this point, (V_E) becomes the exhaust volume (V_{EX}). Hence, due to the changeover operation, an (Exhaust) Gas Recirculation (EGR) process takes within the engine, while the flue gasses are at an elevated pressure. The angular span over which the two ports are open varies between the inlet and the exhaust, in the fashion of the Miller cycle version of the Otto-Diesel engines.

Based on Figure 1, the sequence of events is described below.

Initially (Figure 1(a)), the rotor lobe covers the port leading to the combustion chamber. Theoretically, during this period fuel is injected and combustion takes place within it. In practice, however, this period is far too short for the combustion to be completed in time. In other words, the "combustion chamber" must be composed of a rotating barrel of two or more chambers (at least two or more, depending on the nature of the fuel employed). During the time it takes the lobe to unplug this port, the barrel will rotate and bring forth another cavity, where the combustion has been completed and is ready for expansion. The chamber charged during the previous cycle undergoes a constant volume combustion process. This may be any of the well known Compression Ignition processes (i.e., the standard Compression Ignition of the Diesel engine or the promising Homogeneous Charge, Compression Ignition). At this stage the compression and expansion volumes are equal to zero.

As the shaft turns (Figure 1(b)), the combustion chamber discharges flue gasses into the expansion one, doing work on the rotor. This volume is assembled by the cavity formed by the rotor and the stator as well as the combustion chamber. The starting magnitude of this will be $V_E = V_{CC} = V_5 = V_4$. The subscripts 4 and 5 will become apparent in the description of the thermodynamic cycle, to be given in the next paragraph. Concurrently, compression is implemented inside the corresponding chamber as soon as the opposite lobe tip plugs the inlet port. Similarly for the exhaust.

At a predetermined angular position (Figure 1(c)), diaphragm 1 (which separates the compression from the expansion chamber) is lifted while diaphragm 2 is lowered. The separation between the two chambers is maintained, but now a section ΔV of the previous expansion chamber as well as the combustion volume ($V_{CC} = V_4$) are added to the compression volume. Just before the changeover operation the last had a magnitude $V_C = V_2$. On the other hand, the expansion chamber volume is reduced from a magnitude V_6 to the new (lower) one V_7. In other words, $V_6 = V_7 + \Delta V + V_4$.

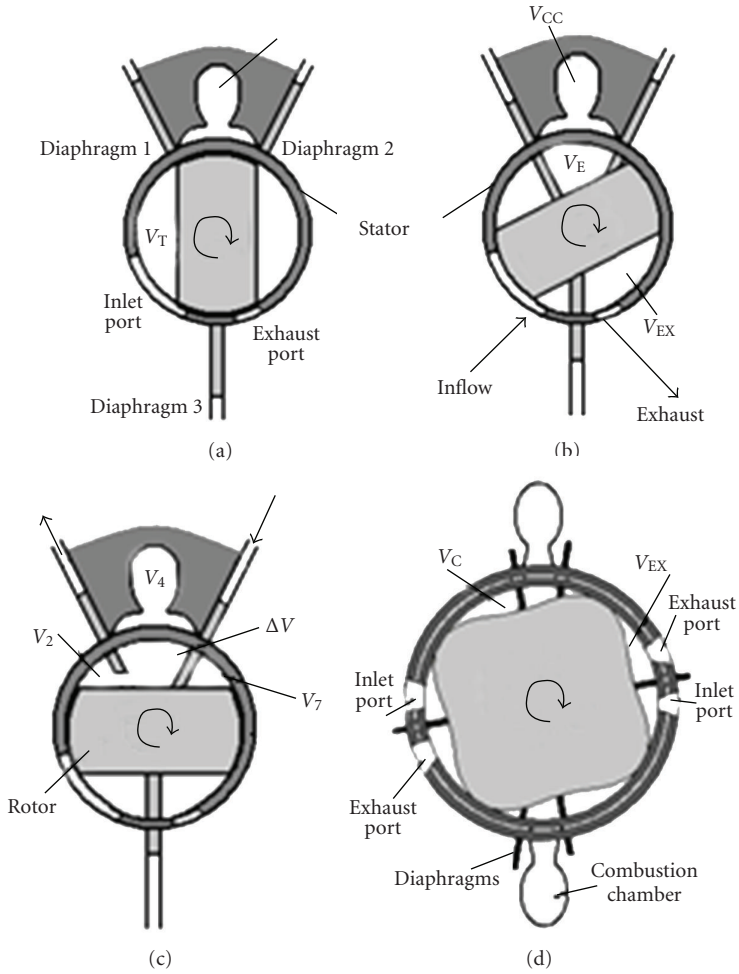

Figure 1: The MG vane rotary engine in cross section (a) closed ports, (b) compression starts, (c) the changeover process, (d) the four lobe version.

The flue gasses in the remaining expansion cavity continue to expand up to the exhaust point (i.e., when $V_E = V_8$). The compression volume is reduced gradually from the combined magnitude $V_C = V_2 + \Delta V + V_4$ to $V_C = V_{CC} = V_4$.

3. The Ideal Thermodynamic Cycle of the MG Engine and Its Reference Counterpart

The operation of the MG concept is based on the thermodynamic cycle illustrated in Figure 2, in both (T-s) and (P-V) axes. The ideal version of the cycle is defined by the cycle station points 1-2-3-4-5-6-7-8-9-1 and is composed of the following processes:

Process (1-2): the fluid is compressed isentropically.

Process (2-3): the fluid at state 2 is mixed with part of the expanding fluid at state 6, due to the changeover. Hence, the compression volume changes from 2 to 3, while the expansion one is reduced from 6 to 7. As a result of the mixing, the fluid properties during the process (2-3) are changed.

Process (3-4): the isentropic compression continues, until it reaches the minimum volume (V_4), which is equal to the volume of the combustion chamber.

Process (5-4): constant volume heating (combustion) takes place.

Process (5-6): isentropic expansion.

Process (6-7): it corresponds to the changeover process. As a result volume and mass are reduced. However, the intensive properties (i.e., temperature, pressure, density, entropy, etc.) of the fluid remain the same.

Process (7-8): the isentropic expansion continues. By proper selection of the inlet-exhaust port arc sizes, the expansion may last longer than the compression, just as in the conventional Miler cycle of the reciprocating engines.

Process (8-9): constant volume cooling up to the atmospheric pressure.

Process (9-1): the fluid is cooled at a constant pressure. In the end it returns to the initial state.

In practice, the last two processes will be replaced by the inlet-exhaust processes. In vane rotary engines, the inlet under pressure and the exhaust overpressure will be smaller when compared against the corresponding processes of the reciprocating engines due to the much larger openings of the inlet-exhaust ports.

The performance of the above cycle is compared against the performance of the ideal Miller cycle employed in modern high efficiency engine (e.g., the slow revving ship Diesel Engines). In Figures 2(a) and 2(b) the last is defined by the station point sequence 1-2M-3M-4M-5M-1 and corresponds to a cycle with the same maximum to minimum temperature ratio (i.e., Θ) and compression ratio (r).

The analysis of the ideal cycle is based on the following assumptions:

(i) the fluid properties remain constant,

(ii) the mass of the fluid changes only due to the EGR.

The analysis is carried out in terms of nondimensional parameters for the pressure (π), the temperature (τ) and the volume (ν). These parameters are derived by dividing the dimensional quantities by the corresponding initial values (at the thermodynamic point 1), that is,

$$\pi_i = \frac{P_i}{P_1}, \qquad \tau_i = \frac{T_i}{T_1}, \qquad \nu_i = \frac{V_i}{V_1}. \tag{1}$$

Parametric analysis in terms of non-dimensional variables constitutes the standard approach (e.g., Kerrebrock [5], Heywood [6], given that such analyses do not provide very accurate quantitative predictions. What they provide is fairly accurate estimates for the influence of variable deviations from a "reference" configuration. A reliable quantitative prediction requires the incorporation of real gas and irreversibility modeling into the cycle analysis, something that is beyond the scope of the present paper.

The following volume restrictions apply.

$$\begin{gathered} V_6 - V_7 = V_3 - V_2 = V_{CC} + \Delta V = V_4 + \lambda V_T, \\ V_9 = \kappa V_T = r_E V_1 = V_8. \end{gathered} \tag{2}$$

The parameter κ defines the maximum "exploitable" section of V_T, since part of it cannot be employed in the compression-expansion processes due to the need for a finite size of the two ports.

$$\begin{gathered} V_6 = V_T + V_4 - V_2, \\ V_5 = V_4. \end{gathered} \tag{3}$$

The volume section transferred during the changeover is determined by the parameter:

$$\lambda = \frac{\Delta V}{V_T}. \tag{4}$$

In addition the following ratios are employed:

$$r = \frac{V_1}{V_4}, \tag{5}$$

$$r_c = \frac{V_1}{V_2}. \tag{6}$$

The ratios r, r_c and r_E are the compression, changeover and overexpansion ratios. The ratio λ will be called "the transferred" volume ratio.

Based upon the above definition and volume restrictions, the non-dimensional versions of the volumes at the corresponding cycle station points are:

$$\begin{gathered} \nu_2 = \frac{V_2}{V_1} = \frac{1}{r_C}, \\ \nu_3 = \frac{V_3}{V_1} = \lambda\left(\frac{r_E}{\kappa}\right) + \left(\frac{1}{r}\right) + \left(\frac{1}{r_C}\right), \\ \nu_4 = \frac{V_4}{V_1} = \frac{1}{r}, \\ \nu_5 = \frac{V_5}{V_1} = \frac{1}{r}, \\ \nu_6 = \frac{V_6}{V_1} = \left(\frac{r_E}{\kappa}\right) + \left(\frac{1}{r}\right) - \left(\frac{1}{r_C}\right), \\ \nu_7 = \left\{\frac{[(1-\lambda)r_E]}{\kappa}\right\} - \left(\frac{1}{r_C}\right) \\ \nu_8 = \nu_9 = r_E \end{gathered} \tag{7}$$

while

$$V_1 = \left(\frac{\kappa}{r_E}\right) V_T \tag{8}$$

The volume transfer that characterizes the processes (2-3) and (6-7) requires that the mass of the fluid inside the volumes during the processes 3-6 is larger that that of the processes 1-2 and 7-9-1. A steady engine operation implies that

$$\begin{gathered} m_1 = m_2 = m_7 = m_8 = m_9, \\ m_3 = m_4 = m_5 = m_6. \end{gathered} \tag{9}$$

Since the intensive fluid properties do not change during the (6-7) process, the mass ratio

$$\frac{m_3}{m_2} = \frac{m_6}{m_7} = \frac{V_6}{V_7}. \tag{10}$$

This means that, once the geometry of the engine has been fixed, so does the above mass ratio. Actually it can easily be shown by a perturbation analysis that if the m_3 mass is perturbed for some reason by Δm_3° (e.g., due a change in the fuel injection), the perturbation will decay through the algorithm

$$\frac{\Delta m_3^{n+1}}{\Delta m_3^\circ} = \left(1 - \left(\frac{V_7}{V_6}\right)\right)^n. \tag{11}$$

The law of energy conservation and the perfect gas assumption imply that

$$\begin{gathered} \tau_3\left(\frac{m_2}{m_3}\right)\tau_2 + \left(1 - \frac{m_7}{m_6}\right)\tau_6, \\ \pi_3 = \left(\frac{m_3}{m_2}\right)\left(\frac{\tau}{\nu_3}\right). \end{gathered} \tag{12}$$

If the maximum temperature ratio ($\Theta = \tau_5$) is fixed as a free design parameter, the isentropic expansion (5-6) gives:

$$\tau_6 = \tau_5\left(\frac{V_5}{V_6}\right)^{\gamma-1} = \Theta\left(\frac{V_5}{V_6}\right)^{\gamma-1},$$
$$\pi_6 = \left(\frac{m_3}{m_2}\right)\left(\frac{\tau_6}{\nu_6}\right), \tag{13}$$

while

$$\pi_3 = \left(\frac{m_3}{m_2}\right)\left(\frac{\tau_5}{\nu_5}\right) = \left(\frac{m_3}{m_2}\right)\Theta r. \tag{14}$$

In addition:

$$\tau_8 = \left(\frac{V_7}{V_8}\right)^{\gamma-1}\tau_7 = \tau_6\left(\frac{\nu_7}{r_E}\right)^{\gamma-1},$$
$$\pi_8 = \frac{\tau_8}{\nu_8}, \tag{15}$$
$$\tau_9 = \tau_8\left(\frac{\pi_9}{\pi_8}\right) = \frac{\tau_8}{\pi_8} = \nu_8 = r_E,$$

since

$$\pi_9 = 1. \tag{16}$$

In a comparison between the MG and the Miller cycles where r, r_E and Θ are the same, it can easily be shown that:

$$\pi_5 = \left(\frac{m_3}{m_2}\right)\pi_{3M} = \left(\frac{m_3}{m_2}\right)\Theta r, \tag{17a}$$

$$\tau_8\frac{\tau_{4M}}{(m_3/m_2)} = \frac{r^{\gamma-1}}{(m_3/m_2)}, \tag{17b}$$

$$\pi_8 = \frac{\pi_{4M}}{(m_3/m_2)^{\gamma-1}}. \tag{17c}$$

In other words, the ideal MG cycle has a higher maximum pressure than the corresponding Miller cycle and smaller exhaust temperature and pressure. The ratios (π_5/π_{3M}), (τ_8/τ_{4M}),and (π_8/π_{4M}) are all functions of the ratio (m_3/m_2). Actually, when $(m_3/m_2) \rightarrow 1$, the MG cycle coincides with the Miller one.

The works transferred during the cycle processes (w) are non-dimensionalized by the quantity $(m_1C_VT_1)$. As an example, for the isentropic compression process (1-2) the non-dimensional work transfer (w_{12}) is equal to

$$w_{12} = \frac{W_{12}}{m_1C_VT_1} = \frac{m_1C_V(T_2 - T_1)}{m_1C_VT_1} = t_2 - 1.$$
$$w_{34} = \left(\frac{m_3}{m_2}\right)(\tau_4 - \tau_3),$$
$$w_{56} = \left(\frac{m_3}{m_2}\right)(\Theta - \tau_6), \tag{18}$$
$$w_{78} = \tau_7 - \tau_8,$$
$$w_{91} = (\gamma - 1)(r_E - 1).$$

SimilarlyThe corresponding heat transfer quantities (q) are non-dimensionalized by the same quantity, so that their non-dimensional counterparts are

$$q_{IN} = q_{45} = \left(\frac{m_3}{m_2}\right)(\Theta - \tau_4),$$
$$q_{OUT\text{-}1} = q_{89} = \tau_8 - \tau_9 - \tau_8 - r_E, \tag{19}$$
$$q_{OUT\text{-}2} = q_{91} = \gamma(\tau_9 - 1) = \gamma(r_E - 1).$$

The thermal efficiency of the MG cycle (η_{MG}) is given by:

$$\eta_{MG} = 1 - \frac{(q_{OUT\text{-}1} + q_{OUT\text{-}2})}{q_{IN}} \tag{20}$$

while the mean effective pressure of the cycle (mep_{MG}) is given by

$$mep_{MG} = \frac{W_T}{P_1(V_9 - V_4)}, \tag{21}$$

where

$$W_T = W_{56} + W_{78} - W_{12} - W_{34} - W_{91} \tag{22}$$

and P is the fluid pressure at state 1.

The efficiency and the mean effective pressure of the Miller cycle are evaluated through a similar procedure.

4. A Parametric Analysis of the Ideal Cycles

The analysis employs Θ, r, r_c, r_E, λ, and κ as free parameters. For current hydrocarbon fuel engines, parameter (Θ) lies within the range $6 \leq \Theta \leq 9$. Parameter r represents the conventional compression ratio. Parameter (r_c) must be located near the optimum efficiency point. Parameter (κ) was taken equal to 0.9, that is, the engine exploits nearly the entire maximum chamber volume at the expansion (before the exhaust hole is uncovered). In the present analysis, (λ) is a free parameter. Parameter (r_E) was fixed so the pressure at station 8 was always above the starting point one (i.e., P_1). This implies that this will be above the atmospheric one (usually).

The (T-s) and (P-V) diagrams of the ideal cycle are illustrated in Figure 2, where the MG cycle is compared against the corresponding Miller one. The parameter (r_c) is near the optimum value. The entropy variation of the GM cycle is larger than that of the Miller. When combustion starts, the temperature (i.e., τ_4) of the GM cycle is much higher than the corresponding value of the Miller cycle. At the optimum (r_c) value the pressures π_2 and π_6 are nearly the same. This implies that the changeover operation will neither induce strong structural vibrations nor external noise. The resulting pressure rise between the points 2 and 3 is not very large. The compression is simply 'elongated' and this results into the larger τ_4 magnitude.

Figure 3 illustrates the influence of the ratio (Θ) on the P-V diagram structure. Although a higher (Θ) induces larger pressures at the expansion, it has a rather small effect on the (π_6) level. In other words, the engine will have a larger

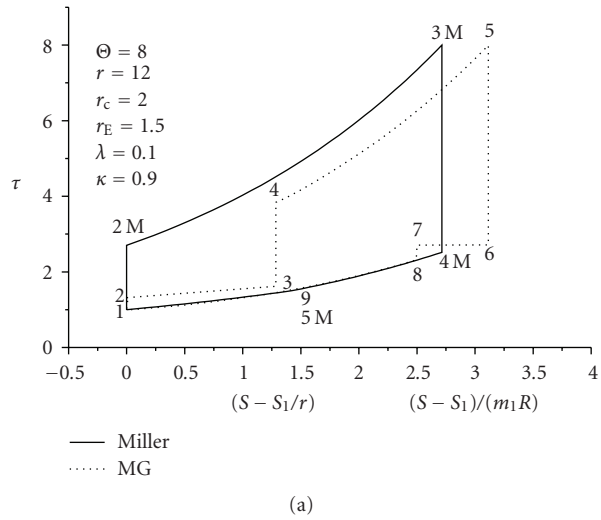

(a)

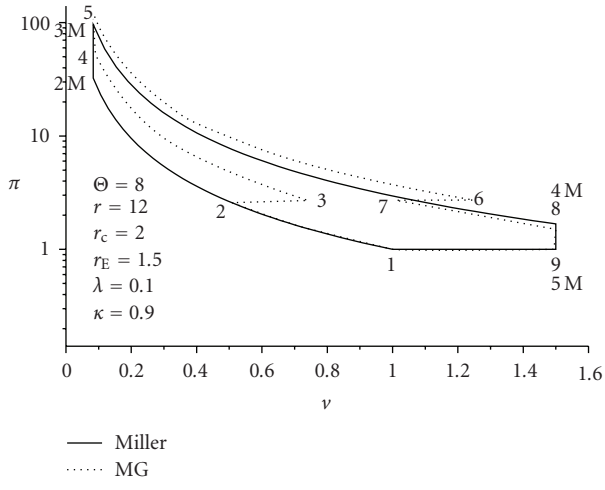

(b)

Figure 2: The MG engine. Thermodynamic cycle and the corresponding Miller one (a) the *T-s* diagram, (b) the *P-V* diagram.

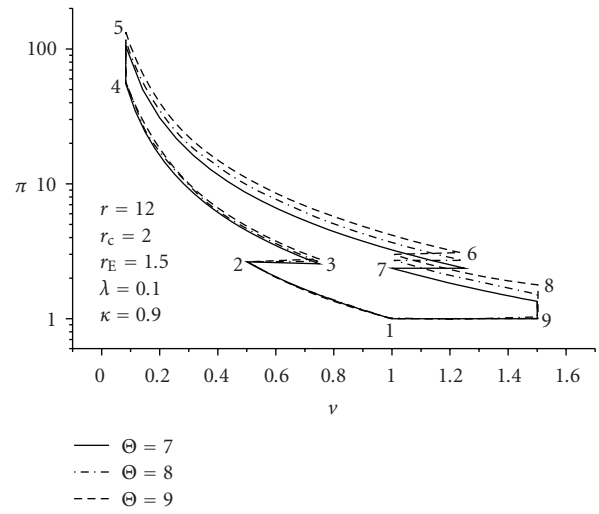

Figure 3: The influence of (Θ) on the *P-V* diagram.

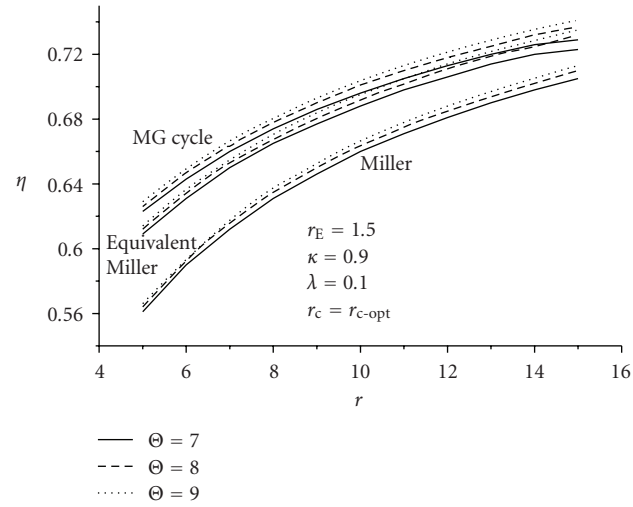

Figure 4: The thermal efficiency against the compression ratio.

mep but the changeover effects will remain moderate, On the other hand, the (Θ) effect upon the compression process is small.

Figure 4 illustrates the influence of the compression ratio on the thermal efficiency for three (Θ) values and when $r_E = 1.5$. The parameter r_c is maintained at the optimum value. The MG cycle has a very clear advantage over the Miller cycle. This efficiency difference is maintained nearly constant for all compression ratios and is of order 4 percentage points, that is, nearly 6% higher than that of the corresponding Miller cycle. This implies that the MG cycle is producing the same efficiency as the Miller cycle at a smaller compression ratio. Since, however, the MG cycle gives a larger maximum pressure than that of the Miller cycle (17a), the concept of the "equivalent" Miller cycle is introduced. This cycle has the same parameters with the MG cycle except for the compression ratio. The last is increased, so that its maximum pressure is the same with that of the MG cycle. The results show that the MG cycle maintains its thermal efficiency advantage. The rest of the analysis on the characteristics of the cycle when $\Theta \leq 6$. This corresponds to maximum cycle temperatures below 1800°K, that is, in a region where the NOx concentrations within the flue gasses are very small.

The parametric analysis employs the following configuration as "reference" point: (i) $\Theta = 6$ (ii) $r_E = 2$, (iii) $\lambda = 0.152$, (iv) $\kappa = 0.9$, (v) $r = 10$. The volume ratio r_c remains a free parameter through.

Figure 5 presents the results for the thermal efficiency against the ratio r_c and a second free parameter, that is, Θ (Figure 5(a)), r (Figure 5(b)) or λ (Figure 5(c)). The calculations showed that:

In all cases, the $\eta_{th} \sim r_c$ relationship exhibits a maximum η_{th} when r_c is of order $r_c = 1.5$.

(i) The magnitude of this optimum r_c point is not affected significantly by the changes in the other free parameters (i.e., Θ, r, λ).

(ii) The cycle exhibits a thermal efficiency of the order of 65–70%.

(iii) In general, the efficiency drops to around 0% when $r_c = 5$ for all the second parameter changes, that is, they reach the ideal Otto cycle efficiency for conventional gasoline engines.

(iv) In general, near the optimum r_c point, the efficiency increases with Θ, r, λ changes. It must be noted that the efficiency remains nearly constant over the entire region $6 \leq \Theta \leq 9$. In other words, the cycle has no need of a very high Θ in order to produce high efficiency levels.

Figure 6 studies the corresponding effects on the cycle mean effective pressure (mep). The Θ variations are by far the most effective in increasing mep, with r second and λ nearly non-effective near the r_c value that gives optimum η_{th} results. This optimum r_c point generates maximum mep values as well, although the magnitude of the mean effective pressure does not vary significantly with r_c. For the "reference" point the non-dimensional mep value was of the order of 6, that is, nearly 2/3 that of a conventional gasoline engine but similar to that of a Miler cycle engine.

Figure 7 studies the effect of the free parameters on the mass recirculation ratio (i.e., m_3/m_2). In general, this ratio decreases with r_c reaching a maximum near the optimum point ($r_c \approx 1.5$). The temperature ratio (Θ) has no influence at all, while the compression ratio (r) exhibits a mild influence. On the other hand, the volume change-over parameter (λ) does affect significantly the mass exchange ratio (as one would expect). For the reference configuration the m_3/m_2 is of order 1.3–1.4, that is, similar to exhaust gas recirculation (EGR) ratios in conventional gasoline engines.

Figure 8 studies the τ_4 ratio. As noted earlier, this ratio gives the temperature at the end of the compression, just before the combustion starts. In highly debuted fuel-air mixtures (as expected in HCCI concepts), this temperature should exceed the level of 1000°K (i.e., $\tau_4 > 3.5$, for inlet air temperatures of the order of 288°K). The analysis of the results indicates that: In order to guarantees for ignition at all conditions, the value of (λ) should be near or above the $\lambda = 0.15$ limit.

At the optimum r_c point the τ_4 reaches a minimum. Thus, in order to facilitate reliable ignition, it would be preferable to design the engines with $r_c \approx 2$ at a small expense of a somewhat reduced thermal efficiency ($\Delta\eta_{th} < 1\%$) and mep (Δmep < 0.2).

5. Conclusions

The present paper investigates the ideal cycle of the Meletis-Georgiou Vane Rotary engine. The analysis establishes the relationships among the main parameters and proceeds to evaluate the merits of the new engine against the corresponding Miller cycle. The results have shown that this cycle has a higher thermal efficiency and mep against the best thermodynamic cycle in application, that is, the Miller extension of the Otto cycle employed in the slow speed

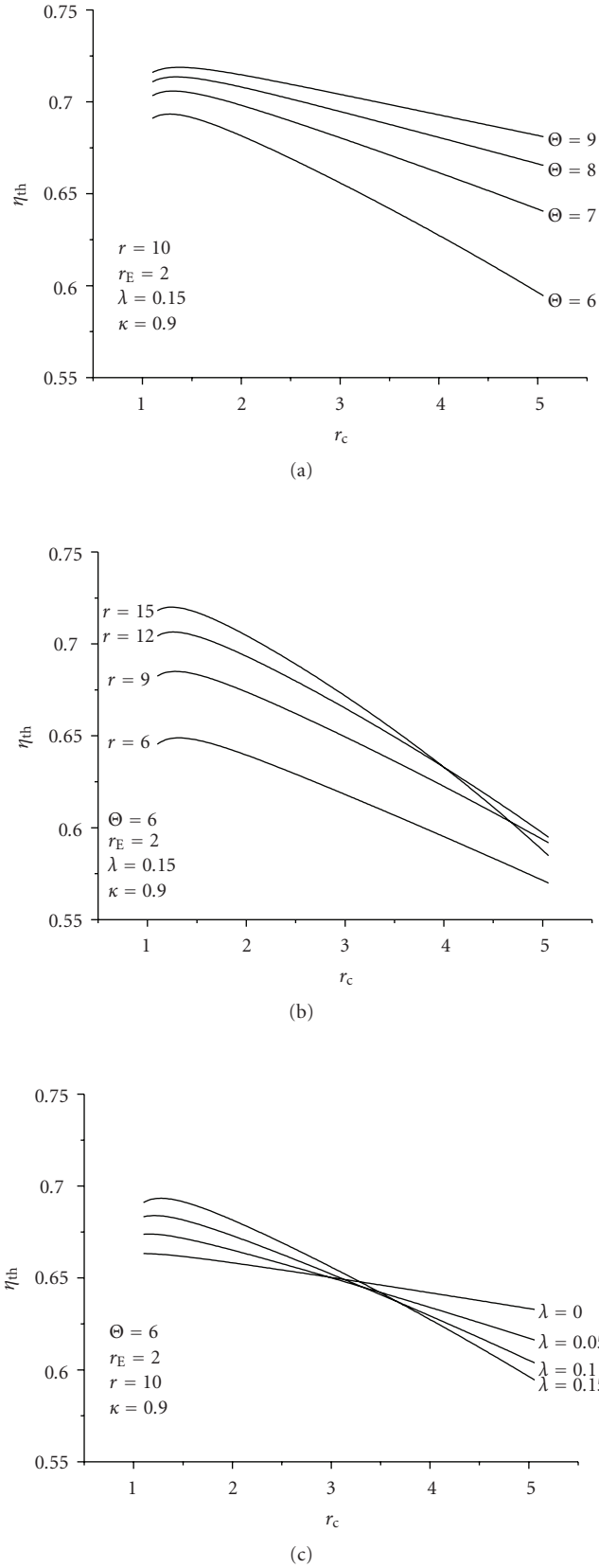

Figure 5: The combined influence of the "volume exchange" ratio (r_c) and the free parameters of (a) the temperature ratio Θ, (b) the "overall compression ratio (r) and (c) the combustion gases mass exchange ratio (λ) on the thermal efficiency of the cycle.

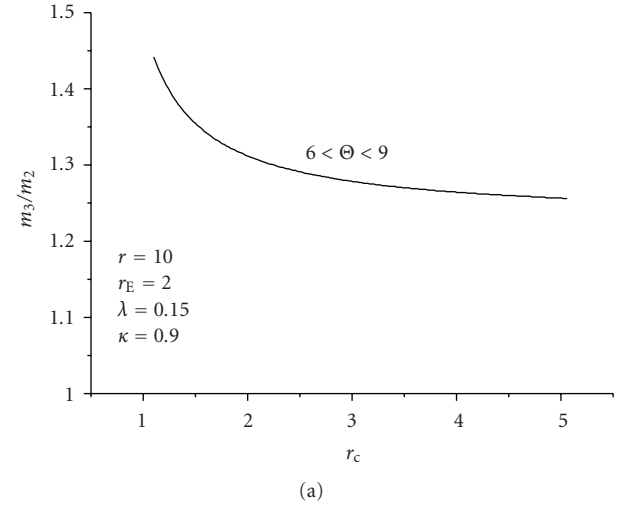

(a)

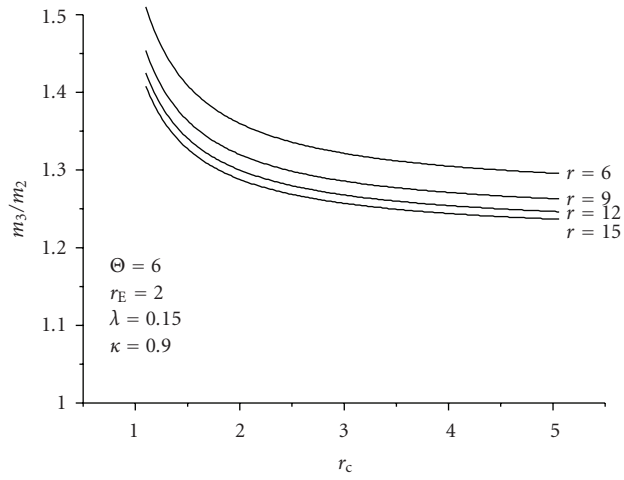

(b)

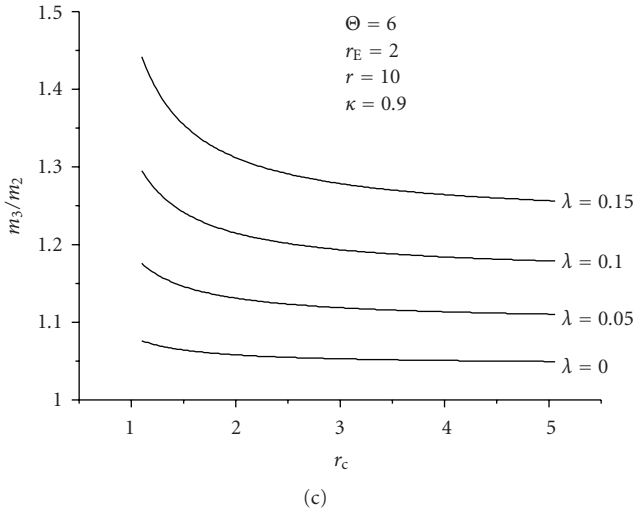

(c)

Figure 6: The combined influence of the "volume exchange" ratio (r_c) and the free parameters of (a) the temperature ratio Θ, (b) the "overall compression ratio (r) and (c) the combustion gases mass exchange ratio (λ) on the gas mass ratio (m_3/m_2) during the exchange process.

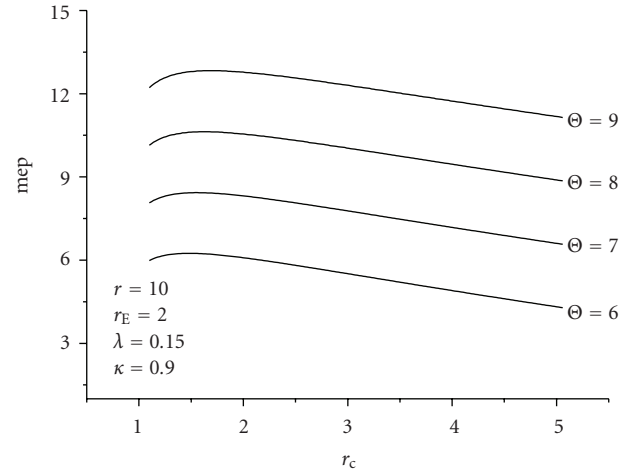

(a)

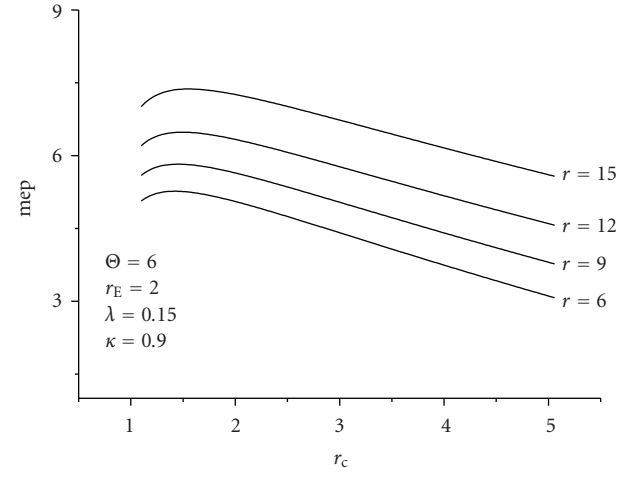

(b)

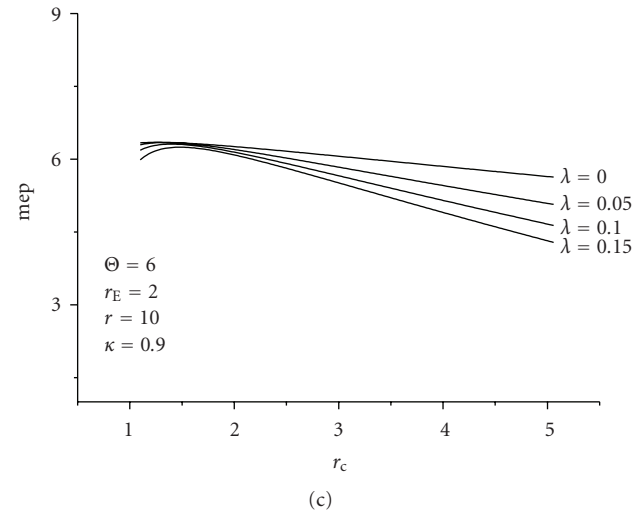

(c)

Figure 7: The combined influence of the "volume exchange" ratio (r_c) and the free parameters of (a) the temperature ratio Θ, (b) the "overall compression ratio (r) and (c) the combustion gases mass exchange ratio (λ) on the mean effective pressure (mep) of the cycle.

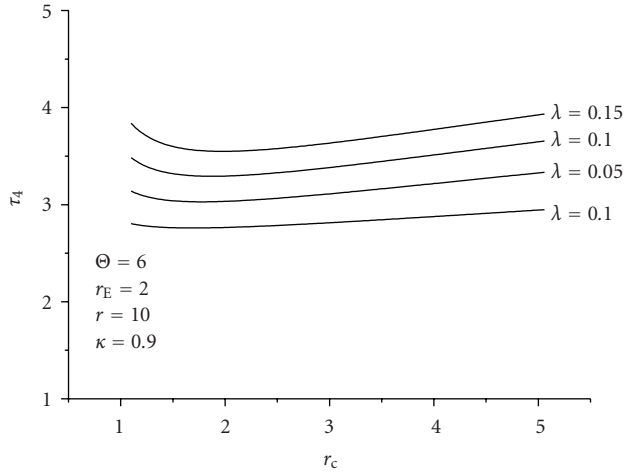

(a)

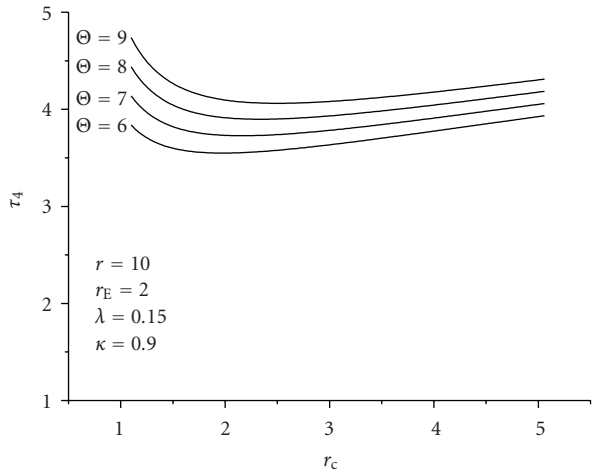

(b)

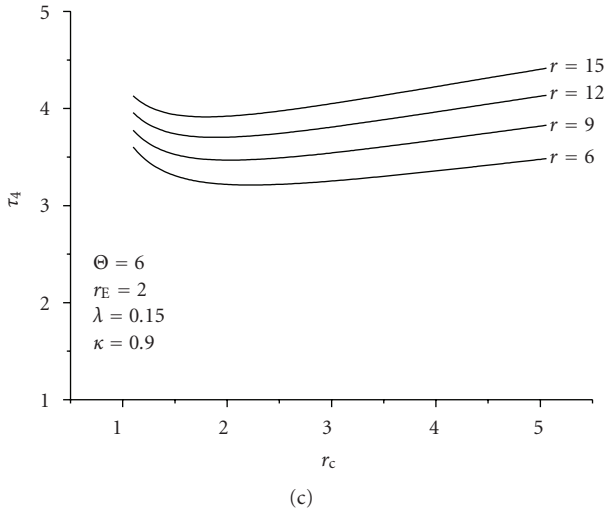

(c)

Figure 8: The combined influence of the "volume exchange" ratio (r_c) and the free parameters of (a) the temperature ratio Θ, (b) the "overall compression ratio (r) and (c) the combustion gases mass exchange ratio (λ) on the temperature ratio (τ_4) at the end of the compression process.

Marine Diesel Engines. At the same time, the temperature at the completion of the compression much closer to that required by Homogeneous Charge Compression Engines than conventional Otto type engines with the same compression ratio.

Nomenclature

English Symbols

VR: Vane Rotary
EGR: Exhaust Gas Recirculation
m: Mass
P: Fluid Pressure
W: Work transferred during the cycle processes
w: Non-dimensional work transfer
r: The compression ratio
r_c: The changeover ratio
r_E: The over-expansion ratio
v_E: The expansion one
V_{EX}: The exhaust one
V_{IN}: The inlet volume
V_C: The compression one
V_{CC}: Combustion volume
V_T: Total volume
mep_{MG}: Mean effective pressure of the cycle.

Greek Symbols

η : Thermal efficiency
Θ : Maximum temperature ratio
τ : Temperature
λ : The transferred volume ratio
v : Volume
π : Pressure.

References

[1] E. Meletis and D. P. Georgiou, "Vaned Rotary Engine with Regenerative Preheating," WPO, no. 98/10172, 12-03-1998.
[2] I. S. Akmandor and N. Ersoz, "Rotary Vane Engine and Thermodynamic cycle," WPO, no. 2004/022919, 18-03-2004.
[3] J. P. Penn, "Radial Vane Rotary Engine," USA Patent Office, no. 5,540,199, 30-07-1996.
[4] C. Yamashina and S. Miyakawa, "Vane type Rotary machine," European Patent Office, no. 1 113 175, 03-09-1999.
[5] J. L. Kerrebrock, *Aircraft Engines and Gas Turbines*, The MIT Press, New York, NY, USA, 2nd edition, 1992.
[6] J. B. Heywood, *Internal Combustion Engine Fundamentals*, McGraw-Hill Book, New York, NY, USA, 1988.